

# Exploration of the Communication Area of Infrared Short-Range Communication Systems for Intervehicle Communication

Wern-Yang Shieh, Hsin-Chuan Chen, Ti-Ho Wang, and Bo-Wei Chen

*Abstract*—Infrared communication in the wavelength band 780-950 nm is very suitable for short-range point-to-point communications. It is a good choice for vehicle-to-vehicle communication in several intelligent-transportation-system (ITS) applications such as cooperative driving, collision warning, and pileup-crash prevention. In this paper, with the aid of a physical model established in our previous works, we explore the communication area of an infrared intervehicle communication system utilizing a typical low-cost commercial light-emitting diodes (LEDs) as the emitter and planar p-i-n photodiodes as the receiver. The radiation pattern of the emitter fabricated by aforementioned LEDs and the receiving pattern of the receiver are approximated by a linear combination of cosine<sup>n</sup> functions. This approximation helps us analyze the system performance easily. Both multilane straight-road conditions and curved-road conditions with various radius of curvature are taken into account. The condition of a small car communicating with a big truck, i.e., there is a vertical mounting height difference between the emitter and the receiver, is also considered. Our results show that the performance of the system meets the requirement of aforementioned ITS applications in terms of the communication area.

*Keywords*—Dedicated short-range communication (DSRC), infrared communication, intervehicle communication, intelligent transportation system (ITS).

## I. INTRODUCTION

**I**NTERVEHICLE communication is essential and even indispensable in many intelligent-transportation-system (ITS) applications such as cooperative driving, collision warning, pileup-crash prevention, and other situations where data transmission between vehicles is necessitated. Currently, microwave in the 2.4-GHz and 5.8-GHz band are considered and designed to serve these applications. These can be seen in many recent literatures such as [1]–[7].

Besides microwaves, infrared light in the wavelength band 780-950 nm also plays an important role in ITS applications [8]–[14], it is especially suitable for short-range point-to-point data transmission. Hence, in many cases it is also a good choice for intervehicle communication and under some circumstances it can compensate for the deficiency of microwave systems, for example, in pileup-crash prevention. In this application, in general, only the vehicles directly in tandem following a car suddenly taking a hard break need

This work was supported by the National Science Council, Republic of China (Taiwan), under Contract NSC100-2221-E-129-012 and NSC101-2221-E-129-013.

W.-Y. Shieh, H.-C. Chen, T.-H. Wang, and Bo-Wei Chen are with the Department of Electronic Engineering, St. John's University, Tamsui District, New Taipei City, Taiwan 25135, R.O.C. (e-mail: shiehwy@mail.sju.edu.tw, robin@mail.sju.edu.tw, dhwang@mail.sju.edu.tw, 99412008@stud.sju.edu.tw)

to receive the information disseminated from that car [3]. However, for microwave systems, generally the transmitted data will be widely sent and inevitably received by vehicles which are irrelevant to that hazardous condition unless the antennas are very carefully designed.

The fact that early warning of the hard break of a vehicle for the other vehicles following behind in tandem, especially for those whose field of vision are blocked, can reduce the possibility of pileup crash is without further discussion. This needs data transmission in the backward direction with limited angular width in order not to send the message to irrelevant vehicles, for instance, those in other traffic lanes. For cooperative driving [1], however, it is also necessary to send the related information, such as intention of changing traffic lane, to the vehicles in adjacent traffic lanes. For these two applications there is a common characteristic—the information should be backwardly transmitted within limited angular width.

In this paper we will explore the performance of an infrared intervehicle communication system in terms of communication area. The system is expected to be valuable for aforementioned ITS applications.

## II. PHYSICAL MODEL OF INFRARED SHORT-RANGE COMMUNICATION SYSTEMS

Figure 1 (a) simply shows the scenario for pile-up-crash prevention, several vehicles traveling in tandem. The message of a sudden break of the first vehicle should be sent to the following vehicles in the same traffic lane, one by one, i.e., the first vehicle sends the message to the second, the second receives and notices this message, at the same time transmits it to the third, the third receives and transmits it again to the fourth, and so forth. In this procedure, the number of transmissions can be counted, and the transmission can be stopped after a preselected number of times. Now, in addition to the simplest condition sketched in Fig. 1 (b), which shows two vehicles in tandem communicating each other, our concern is the performance of the communication system in terms of the communication area under different circumstances such as the vehicles traveling on curved roads and for different heights of the vehicles as shown in Figs. 1 (c) and (d). For cooperative driving, the related message has also to be sent to the vehicles in contiguous traffic lanes as displayed in Fig. 1 (e). Hence, this condition is also considered in this paper.

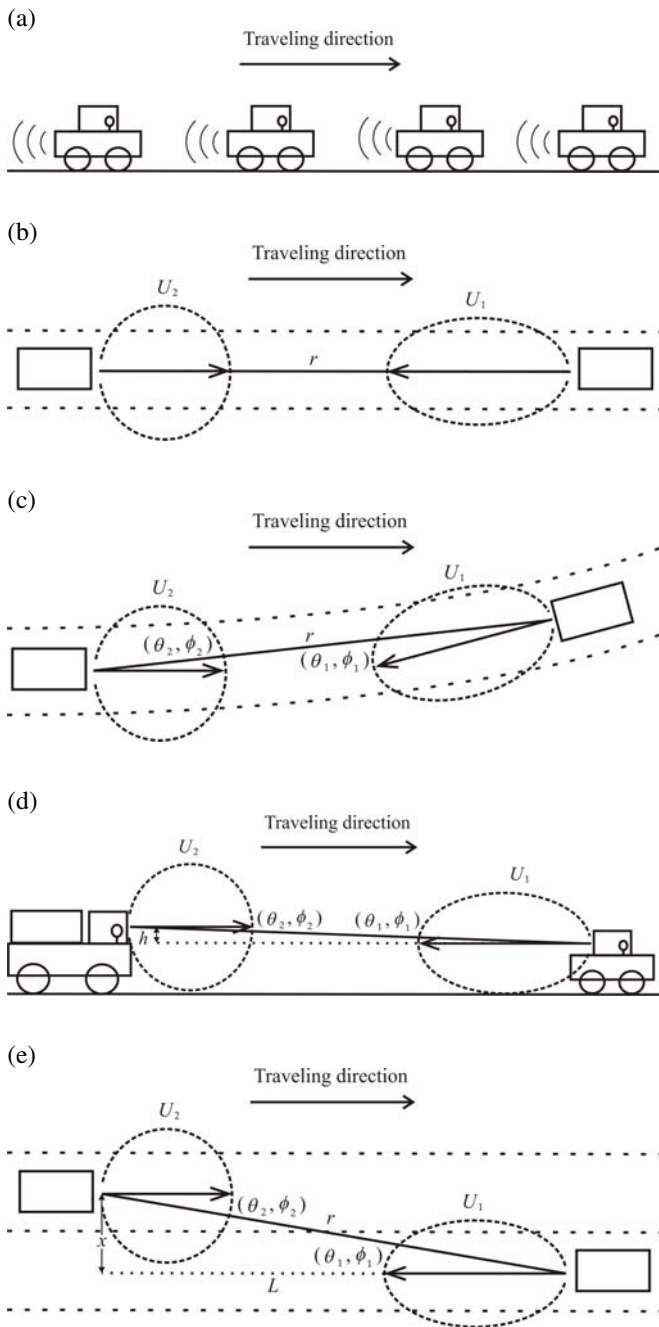


Fig. 1. (a) Several vehicles traveling in tandem, (b) two vehicles traveling in the same traffic lane communicating each other, (c) two vehicles traveling on a curved road communicating each other, (d) two vehicles with different heights communicating each other, (e) two vehicles in adjacent traffic lanes communicating each other.

### A. Brief Review of the Physical Model

The physical model for infrared short-range communication systems utilizing light-emitting diodes (LEDs) and p-i-n photodiodes, respectively, as emitting and receiving components has been established in our previous works for electronic-toll-collection (ETC) applications [9]–[14]. That model can be used to our current application, i.e., intervehicle communication, without any difficulty. The signal strength received by

the receiver and emitted by the emitter can be described by

$$S = A_0 \frac{U_1(\theta_1, \phi_1) U_2(\theta_2, \phi_2)}{r^2}, \quad (1)$$

where  $A_0$  is the amplitude constant,  $U_1(\theta_1, \phi_1)$  is the radiation pattern of the emitter,  $U_2(\theta_2, \phi_2)$  is the receiving pattern of the receiver, and  $r$  is the distance between the emitter and the receiver.  $U_1$  and  $U_2$  are functions of emitting direction  $(\theta_1, \phi_1)$  and receiving direction  $(\theta_2, \phi_2)$ , respectively, where  $\theta_1, \phi_1$ , and  $\theta_2, \phi_2$  are defined following the conventional spherical polar coordinates relative to the normal of the corresponding module, i.e., the emitter and the receiver. The meaning of  $\theta_1, \phi_1$  and  $\theta_2, \phi_2$  can be seen in Figs. 1 (c), (d), and (e).

For infrared communication systems, p-i-n photodiodes are very often used as the signal detector. In our systems we utilized planar p-i-n photodiodes as the receiver, whose receiving pattern can be described with high precision by a simple cosine function, i.e.,  $\cos \theta$ , where  $\theta$  is the incident angle of the signal relative to the normal of the diode facet. This means that for our physical model in (1) the receiving pattern of the receiver can be described by

$$U_2(\theta_2, \phi_2) = \cos \theta_2.$$

The sketch of this pattern has appeared in our previous work (see Fig. 3 in [9]). Over the past years we have also measured the receiving pattern of several such p-i-n photodiodes. The results did not contradict the use of  $\cos \theta$  to approximate their receiving patterns.

### B. Radiation Pattern of the Emitter

To send the signal into desired directions and obtain a communication area suitable for our specific purposes, the radiation pattern of the constituent LEDs of the emitter should be appropriate. For our applications, the communication range of the system should reach at least several tens of meters in the longitudinal direction, i.e., in the vehicle traveling direction, and in the lateral direction the communication area should cover adjacent traffic lanes. To fulfill this requirement, the half-intensity angle of the emitter should be near  $10^\circ$ , i.e.,  $\Phi_{1/2} \sim 10^\circ$ . However, according to our measurements, most low-cost commercial infrared LEDs are unsuitable due to their irregular radiation patterns [12].

Because till now we cannot find any LED with both a suitable half-intensity angle and a regular radiation pattern, hence, we have to choose marginally acceptable ones [12]–[14]. From such huge amount of commercial LEDs, taking account of the half-intensity angle and the extent of the irregularity of its radiation pattern, and partly because of its low cost, we selected a type named TSFF5200 fabricated by a world renown company to construct our emitter. The specification of this LED can be found in the data sheet provided by the manufacturer [15]. According to the data sheet, its half-intensity angle is  $\Phi_{1/2} = 10^\circ$ . We have very carefully measured the radiation patterns of many individual diodes of this type of LEDs. Figure 2 (solid line) is a typical result depicted in [10], some others can also be found in [13], [14]. As shown in Fig. 2, the radiation patterns of this type of LEDs have a common irregular characteristic—a notch in

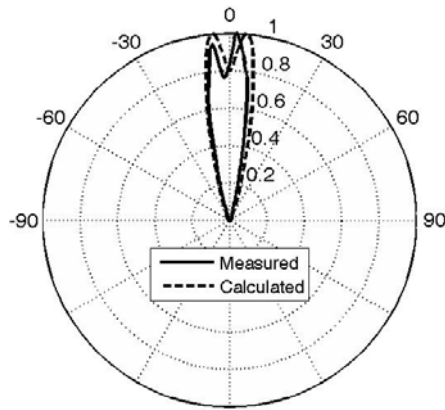


Fig. 2. Measured (solid line) and calculated (dashed line) radiation pattern of the TSFF5200 LED along a definite azimuthal angle.

the central radiant direction. Our measured results reveal that the depth of the notch is different from diode to diode, from about 15% to 25%, and there exist noticeable discrepancies between the radiation patterns of the individual LEDs even they are coming from the same manufacturing lot [10], [13], [14].

Despite the aforementioned disparities between the radiation patterns of individual diodes of this type of LEDs, such irregular patterns can be approximated by

$$U_{5200} = 1.0783 (\cos^{45}\theta - 0.45 \cos^{284}\theta) \quad (2)$$

with acceptable agreement [10], [13], [14]. This approximation is based upon the following assumptions

- 1) half-intensity angle  $\Phi_{1/2} = 10^\circ$ ,
- 2) a 20% notch in the central radiant direction, and
- 3) the patterns are axial symmetric.

In Fig. 2, the dashed line is the calculated result by using this approximation. Although the approximation (2) is not very precise for the pattern of each individual LED, however, for an emitter fabricated with several number of such LEDs in an unidirectional array [10], this approximation is very close to the reality when the number utilized is increased. The reason is the somewhat randomness of the pattern of each individual LED—nearly every one has a 15% to 25% notch, the position of the deepest point of the notch is different from diode to diode, scattering in a few degree (most of them within  $5^\circ$ ) around the physical symmetric axis of the diode. Hence, when many of them sum up, the result approaches the approximation (2). Figure 3 shows the measured three-dimensional radiation patterns of two emitters fabricated by (a) twelve and (b) twenty TSFF5200 LEDs, respectively, in a unidirectional array, the component LEDs of the emitters were randomly selected. Following the conventional definition of the spherical-polar coordinates, in the figures in Fig. 3  $\theta'$  is the polar angle relative to the  $z'$ -axis, which is indicated by the red vertical line corresponding to the physical symmetric axis of the LEDs, and  $\phi'$  is the azimuthal angle relative to the  $x'$ -axis of the emitter, which is the  $\phi' = 0$  line in the figures. For clarity, we only show one half of the measured results, i.e.,  $90^\circ \leq \phi' \leq 180^\circ$  and  $-90^\circ \leq \phi' \leq 0^\circ$ . The

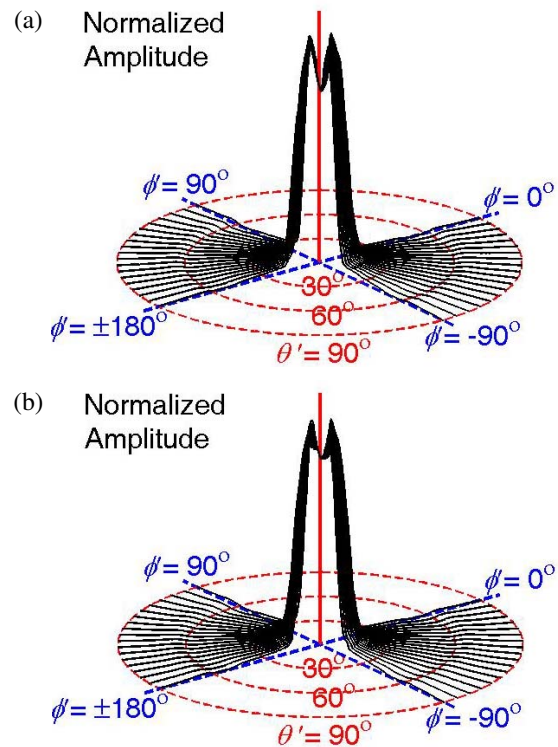


Fig. 3. Measured three-dimensional radiation pattern of the emitter fabricated with (a) twelve and (b) twenty TSFF5200 LEDs.

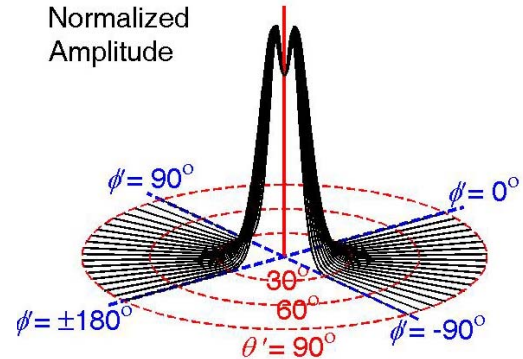


Fig. 4. Calculated radiation pattern of TSFF5200 LED.

results of the other half are similar, therefore are omitted here. The measured results reveal that the radiation patterns of these two emitters are very close to axial symmetric. In the central radiant direction the emitter with twelve LEDs has a 20% notch, and that with twenty LEDs has a 16% notch. Figure 4 is the calculated result by using approximation (2). Comparing Figs. 3 and 4, it is clear that they are in quite good agreement, despite the fact that the notch of the emitter with twenty LEDs is slightly shallower than that of the calculated result. Notice that the depth of the notch of some of the measured radiation patterns of individual LEDs can be as deep as 25%. Therefore we still utilize approximation (2) to analyze the system in order to obtain conservative results, i.e., when the emitter is composed of more than ten LEDs in a unidirectional

array, the radiation pattern of the emitter will have very little probability having a notch deeper than the calculated result of 20%.

### III. COMMUNICATION AREA OF THE SYSTEM

In our previous works we have designed several emitters for ETC applications, each provides its specific system performance in terms of the spatial distribution of signal power. For different distribution of signal power, the system has different communication area and different ability to withstand signal attenuation [9]–[14]. For the convenience of comparison, all of them were assumed to emit the same total radiant power under the same operating conditions. Owing to the ETC applications, they were designed mainly for communication range within twenty meters. To meet the requirement of intervehicle communication for our current purposes, the communication range of the system has to reach several tens of meters. This can be achieved by raising the *effective power* of the system. This means that one can simply increase the power of the emitter, and/or redesign the modulating and demodulating scheme and related circuits. In any case the aforementioned physical model established in our previous works [9]–[14] can be utilized here for analysis without any difficulty.

Based on the aforementioned physical model [9]–[14], for our current application, the normalized signal strength emitted by the emitter and received by the receiver can be described by

$$S_n = \frac{20000}{9} \frac{4.6 U_{5200}(\theta_1) \cos \theta_2}{r^2}, \quad (3)$$

where, as mentioned earlier,  $\cos \theta_2$  is the receiving pattern of the receiver, the constant 4.6 is used to adjust the output power of the LEDs such that all the LEDs emit the same total radiant power irrespective of their radiation patterns in our design, and the constant  $20000/9$  was decided by a technique called *arbitrary scale* [9], which leads to the result that when  $S_n > 1$  the data transmission can be successful, otherwise it fails. The arbitrary-scale technique is fulfilled with the aid of a measurement of the available communication length of the system under a certain configuration. This measured communication length can be used to determine the communication boundary. Then in the analysis we compare all the received signal strengths with that of the communication boundary, whose value was normalized to 1. The details of all these discussions can be found in our previous works [9]–[12], especially in [9]. Comparing the value  $20000/9$  used here in (3) with the value  $1000/9$  appeared in our previous works [9]–[14], it is clear that the effective signal power of current system is 20 times stronger than that of our previous systems for ETC applications.

#### A. Multilane Straight-Road Conditions

For multilane straight-road conditions the vehicles travel along straight traffic lanes as shown in Fig. 1 (e), which shows two vehicles communicating each other with a lateral distance  $x$  and a longitudinal distance  $L$ . There may also exist a vertical height  $h$  between the emitter and the receiver as sketched in Fig. 1 (d). In our analysis we set the receiver located at the

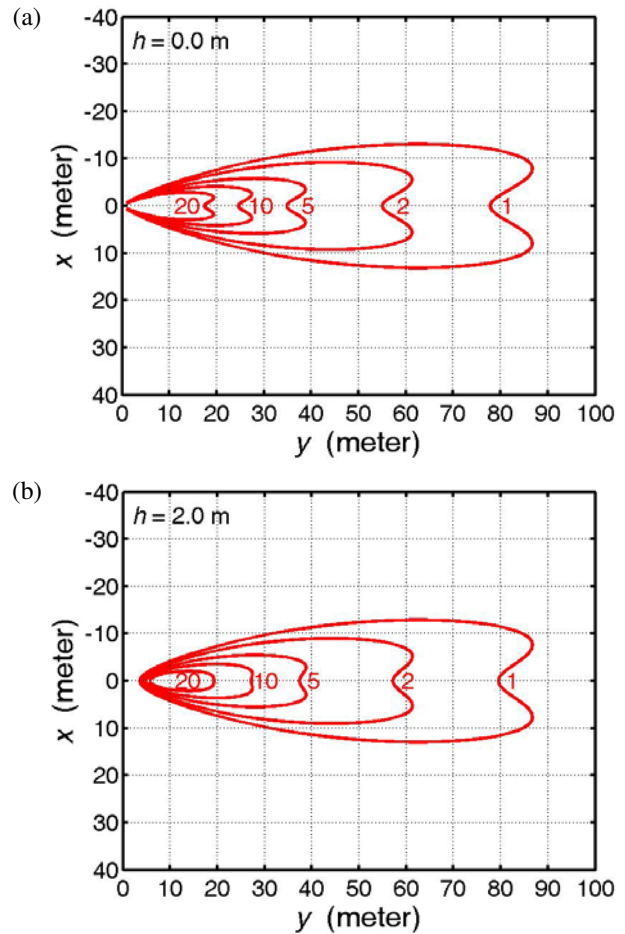


Fig. 5. The contours of the calculated normalized signal strength received by the receiver and emitted by the emitter as a function of the position of the emitter for (a)  $h = 0$  m and (b)  $h = 2$  m, under multilane straight-road conditions.

origin, then the coordinates of the emitter can be described by  $(x, y, h)$ , where  $y = L$ .

Figures 5 (a) and (b) show the contours of the normalized signal strength received by the receiver and emitted by the emitter as a function of the position of the emitter calculated by using (3), for  $h = 0$  m and 2 m, respectively. In these figures the numbers 1, 2, 5, 10, and 20 indicate the value of the normalized received signal strength. For example, the number "5" means the receiver receives a signal five times stronger than that received at the communication boundary where the received signal strength is indicated by a "1". From these two figures it is clear that the communication area of the system simply reflects the radiation pattern of the emitter—a notch in the central direction in the far region. In addition, as revealed in Fig. 5 (b) for  $h = 2$  m, which simulates the condition of a small car communicating with a big truck, the influence of the vertical height difference  $h$  between the emitter and the receiver is serious only within very near region of a few meters ( $y < 4$  m), where the small car and the big truck are very close and the receiver is off the signal direction of the emitter, hence it cannot receive the signal. From these two figures it is not difficult to realize that for this very simple



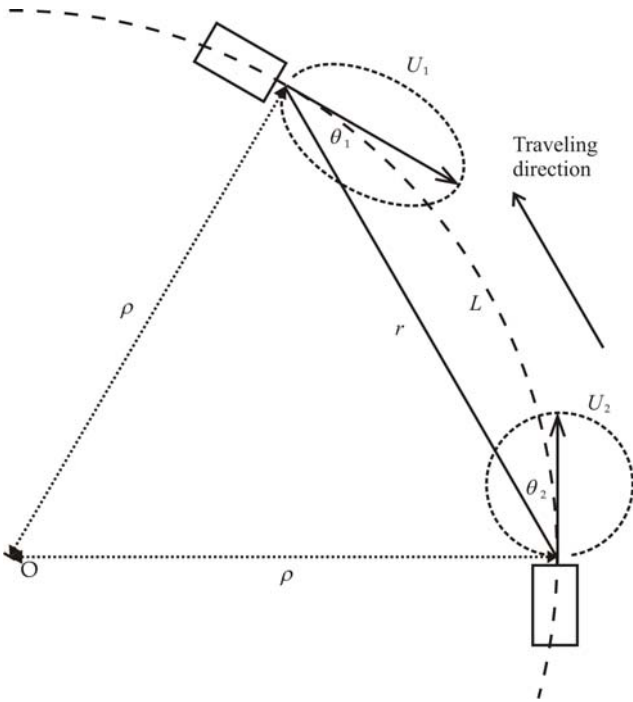


Fig. 6. Vehicles traveling on a curved road with radius of curvature  $\rho$  communicating each other.

emitter and our assumed signal power, two vehicles traveling in the same traffic lane can communicate each other within a range of 77 m without difficulty. For two vehicles traveling in contiguous traffic lanes as in Fig. 1 (e) with a lateral distance  $x = 5.0$  m, these two vehicles can communicate each other when the leading vehicle is in the range from  $y = 11.0$  m to  $y = 84.4$  m, i.e.,  $11.0 \text{ m} < y < 84.4 \text{ m}$ . If these two vehicles are separated by a traffic lane with a lateral distance  $x = 10.0$  m, the communication can be successful when the leading vehicle traveling within the range  $30.3 \text{ m} < y < 85.0 \text{ m}$  ahead. For vehicles separated laterally by  $x > 13.0$  m, it is impossible for them to communicate by using this system for this typical signal power.

For vehicle-to-vehicle communication under normal circumstances, very rarely the longitudinal distance  $L$  between the vehicles will be shorter than 4 m. Hence, the mounting height difference  $h$  between the emitter and the receiver has little adverse influence as far as the communication between the vehicles is concerned.

### B. Curved-Road Conditions

Figure 6 shows the condition for vehicles traveling on a curved road with a radius of curvature  $\rho$ , wherein  $L$  is the distance between the vehicles along the curved road. For the emitter and the receiver mounted at the same height, i.e.,  $h = 0$  m, the distance  $r$  between the emitter and the receiver can be easily obtained by using the cosine law, which reads as

$$r^2 = 2\rho^2 - 2\rho^2 \cos\left(\frac{L}{\rho}\right), \quad (4)$$

and the emitting angle  $\theta_1$  of the emitter and the receiving angle  $\theta_2$  of the receiver relative to the normal of the corresponding

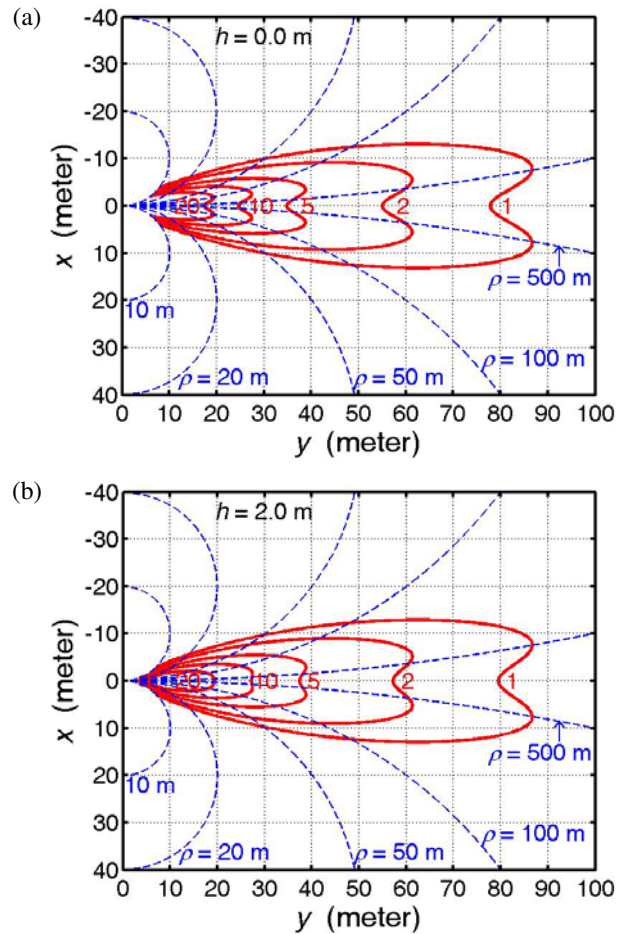


Fig. 7. The contours of the calculated normalized signal strength received by the receiver and emitted by the emitter as a function of the position of the emitter for (a)  $h = 0$  m and (b)  $h = 2$  m under curved-road conditions.

module are

$$\theta_1 = \theta_2 = \frac{L}{2\rho}. \quad (5)$$

For the emitter and the receiver mounted with a vertical height difference  $h$ , the distance  $r$  between the emitter and the receiver can be described as

$$r^2 = 2\rho^2 - 2\rho^2 \cos\left(\frac{L}{\rho}\right) + h^2, \quad (6)$$

and

$$\theta_1 = \theta_2 = \cos^{-1} \left[ \frac{r}{(r^2 + h^2)^{\frac{1}{2}}} \cos\left(\frac{L}{2\rho}\right) \right]. \quad (7)$$

In this analysis we ignore  $\phi_1$  and  $\phi_2$  because we assume that the radiation pattern and the receiving pattern of our modules are axial symmetric. Substituting  $r$ ,  $\theta_1$ , and  $\theta_2$  into (3) we can analyze the conditions for vehicles traveling on curved roads with various radius of curvature easily.

Figures 7(a) and (b) show the contours of the calculated normalized signal strength received by the receiver and emitted by the emitter as a function of the position of the emitter for vehicles traveling on curved roads with various radius of curvature  $\rho$ , for  $h = 0$  m and 2 m, respectively. In these

two figures we utilized thin, blue, curved, dashed lines to indicate the roads with radius of curvature  $\rho = 10, 20, 50, 100,$  and  $500$  m. Comparing Figs. 7 and 5, it is clear that for vehicles traveling on a highway, where the radius of curvature is generally very large ( $\rho > 500$  m), the curved road has little influence on the communication. For a curved road with a radius of curvature  $\rho = 100$  m, two vehicles traveling on the same traffic lane can communicate each other without difficulty when the distance  $L$  between them along the road is shorter than  $50.5$  m, i.e.,  $L < 50.5$  m. For smaller radius of curvature  $\rho = 50, 20,$  and  $10$  m, they can communicate each other only when they are very near within a range of  $L < 32.1$  m,  $L < 16.0$  m, and  $L < 9.1$  m, respectively. From Figs. 7(a) and (b) it is also clear that for a small car communicating with a big truck ( $h = 2$  m) the influence of the vertical mounting height difference  $h$  between the emitter and the receiver on the communication is serious only within very near region, i.e., when the distance  $L$  between the vehicles is shorter than  $4$  m ( $L < 4$  m). Hence, similar to the multilane straight-road conditions, the vertical mounting height difference  $h$  between the emitter and the receiver has little adverse influence on the communication.

#### IV. CONCLUSIONS

Infrared communication in the wavelength band  $780$ - $950$  nm is very suitable for short-range point-to-point communications. It is a good choice for vehicle-to-vehicle communication in several ITS applications such as cooperative driving, collision warning, and pileup-crash prevention. For these applications LEDs with a half-intensity angle  $\Phi_{1/2} \sim 10^\circ$  are beneficial because by using such LEDs it is easy to design suitable communication areas to meet the requirements of the applications. However, the radiation pattern of most low-cost commercial LEDs are irregular to some extent. Thanks to the fact that for any type of LEDs, because of its specific manufacturing procedure, the irregular radiation patterns of individual LEDs reveal a definite characteristic belonging to this type [12]. Hence when many of them sum up, i.e., several LEDs in a unidirectional array, the resultant pattern will converge to a specific irregularity. It is not difficult to obtain a good approximation for this irregular pattern by using a linear combination of cosine<sup>n</sup> functions. In this paper, an infrared intervehicle communication system utilizing a typical low-cost commercial LEDs and planar p-i-n photodiodes as emitter and receiver is analyzed. Owing to the irregular radiation pattern, the emitter fabricated with several TSFF5200 LEDs in a unidirectional array provides a "heart-like" communication area, i.e., a notch in the far region. Roughly estimated, the communication area of the system has a longitudinal to lateral dimension ratio of  $80:25$  for intervehicle communications. Certainly, the communication range of the system depends on the power emitted by the emitter, which can be decided and designed for any specific application. For our typical signal power, the system can provide a communication range of  $80$  m in the longitudinal direction when the lateral distance between the vehicles is shorter than  $12$  m. The communication area for curved-road conditions is similar to that of multilane straight-road

conditions. As expected, the communication range reduces for small radius of curvature. For a small car communicating with a big truck, because very rarely the distance between the communicating vehicles will be shorter than  $4$  m, the mounting height difference  $h$  between the emitter and the receiver has little adverse influence as far as the communication between the vehicles is concerned. Our analyzed results show that the system meets the requirement of several ITS applications in terms of communication area.

#### ACKNOWLEDGMENT

The authors are grateful to the National Center for High-Performance Computing for its support of facilities and software.

#### REFERENCES

- [1] S. Kato, S. Tsugawa, K. Tokuda, T. Matsui, and H. Fujii, "Vehicle control algorithms for cooperative driving with automated vehicles and intervehicle communications", *IEEE Trans. Intell. Transport. Syst.*, vol. 3, pp. 155–161, Sep. 2002.
- [2] H.-S. Tan and J. Huang, "DGPS-based vehicle-to-vehicle cooperative collision warning: engineering feasibility viewpoints", *IEEE Trans. Intell. Transport. Syst.*, vol. 7, pp. 415–428, Dec. 2006.
- [3] A. Chakravarthy, K. Song, and E. Feron, "Preventing automotive pileup crashes in mixed-communication environments", *IEEE Trans. Intell. Transport. Syst.*, vol. 10, pp. 211–225, June 2009.
- [4] C. E. Palazzi, M. Rocchetti, and S. Ferretti, "An intervehicular communication architecture for safety and entertainment", *IEEE Trans. Intell. Transport. Syst.*, vol. 11, pp. 90–99, Mar. 2010.
- [5] A. Kesting, M. Treiber, and D. Helbing, "Connectivity statistics of store-and-forward intervehicle communication", *IEEE Trans. Intell. Transport. Syst.*, vol. 11, pp. 172–181, Mar. 2010.
- [6] G. K. Mitropoulos, I. S. Karanasiou, A. Hinsberger, F. Aguado-Agelet, H. Wieker, H.-J. Hilt, S. Mammari, and G. Noecker, "Wireless local danger warning: cooperative foresighted driving using intervehicle communication", *IEEE Trans. Intell. Transport. Syst.*, vol. 11, pp. 539–553, Sep. 2010.
- [7] N. M. Drawil and O. Basir, "Intervehicle-communication-assisted localization", *IEEE Trans. Intell. Transport. Syst.*, vol. 11, pp. 678–691, Sep. 2010.
- [8] J. S. Kwak and J. H. Lee, "Infrared transmission for intervehicle ranging and vehicle-to-roadside communication systems using spread-spectrum technique", , vol. 5, pp. 12–19, March 2004.
- [9] W.-Y. Shieh, W.-H. Lee, S.-L. Tung, B.-S. Jeng, and C.-H. Liu, "Analysis of the optimum configuration of roadside units and onboard units in dedicated short-range communication systems", *IEEE Trans. Intell. Transport. Syst.*, vol. 7, pp. 565–571, Dec. 2006.
- [10] W.-Y. Shieh, T.-H. Wang, Y.-H. Chou, and C.-C. Huang, "Design of the radiation pattern of infrared short-range communication systems for electronic-toll-collection applications", *IEEE Trans. Intell. Transport. Syst.*, vol. 9, pp. 548–558, Sep. 2008.
- [11] W.-Y. Shieh, C.-C. Hsu, S.-L. Tung, P.-W. Lu, T.-H. Wang, and S.-L. Chang, "Design of infrared electronic-toll-collection systems with extended communication areas and performance of data transmission", *IEEE Trans. Intell. Transport. Syst.*, vol. 12, pp. 25–35, Mar. 2011.
- [12] W.-Y. Shieh, C.-C. Hsu, and T.-H. Wang, "A problem of infrared electronic-toll-collection systems: the irregularity of LED radiation pattern and emitter design", *IEEE Trans. Intell. Transport. Syst.*, vol. 12, pp. 152–163, Mar. 2011.
- [13] W.-Y. Shieh, T.-H. Wang, H.-F. Lin, J.-Y. Chang, and C.-H. Lin, "Design of infrared electronic-toll-collection systems with LEDs with irregular radiation pattern", in *Proc. 2011 IEEE Int. Conf. on Veh. Electro. and Safe.*, Beijing, China, July 10–12, 2011, pp. 124–129.
- [14] W.-Y. Shieh, H.-C. Chen, and T.-H. Wang, "A method to withstand high signal attenuation for infrared electronic-toll-collection systems—equivalent strength of the received signal in the communication area", in *Proc. 2012 IEEE International Conference on Vehicular Electronics and Safety (ICVES12)*, Istanbul, Turkey, July 24–27, 2012, pp.223–227.
- [15] *Datasheet of TSFF5200 High Speed Infrared Emitting Diode, 870 nm, GaAlAs Double Hetero*, Mar. 2005. The Vishay website, 81060.pdf. [Online]. Available: <http://www.vishay.com/docs/81060/>